MR Properties of Excised Neural Tissue Following Experimentally Induced Inflammation

Greg J. Stanisz,[1,2]* Stephanie Webb,[1] Catherine A. Munro,[3] Teresa Pun,[1] and Rajiv Midha[3,4]

Changes in the MR parameters of inflamed neural tissue were measured in vitro. Tumor necrosis factor-alpha (TNF-α) was injected into rat sciatic nerves to induce inflammation with negligible axonal loss and demyelination. The MR parameters, such as T_1/T_2 relaxation and magnetization transfer (MT), were measured 2 days after TNF-α injection and were found to be substantially different from those of normal nerves. The average T_1/T_2 relaxation times increased, whereas the MT ratio (MTR) and the quantitative MT parameter M_{0B} (which describes the semisolid pool of protons) decreased. The MR parameters correlated very well with the extracellular volume fraction (EM) of neural tissue evaluated by quantitative histopathology. The multicomponent T_2 relaxation was shown to provide the best quantitative assessment of changes in neural tissue microstructure, and allowed us to distinguish between the processes of inflammation and demyelination. In comparison, the MT measurements were less successful due to competing contributions of demyelination and pH-sensitive changes in the MT effect. Magn Reson Med 51: 473–479, 2004. © 2004 Wiley-Liss, Inc.

Key words: inflammation; Lewis rat; MRI; magnetization transfer; rat sciatic nerve; TNF-α; T_1; T_2; MTR

Inflammation commonly occurs in a wide spectrum of nervous system diseases, including multiple sclerosis (MS) (1), stroke (2), dementia (3), and traumatic brain injury (4). It is difficult to distinguish the processes of inflammation from those of neural tissue degeneration, such as axonal loss and demyelination, because similar qualitative changes occur in the MR signal intensities of T_1-, T_2-, or magnetization transfer (MT)-weighted images. MRI evaluations of tissue pathology are further complicated by the fact that inflammation, axonal loss, and demyelination often occur concurrently. The precise identification of the pathophysiological processes that occur in nervous system disorders is of considerable importance in our ability to accurately diagnose disease, understand the mechanisms and dynamics of neural tissue degeneration, and evaluate treatment efficacy. There is, therefore, a great need to establish MRI protocols that are capable of differentiating and quantitatively assessing these pathologies.

Quantitative MR measures are thought to provide more specific information about changes in tissue microstructure. For example, the multicomponent T_2 relaxation is sensitive to white matter (WM) demyelination in multiple sclerosis (MS). The observed short T_2 component, which occurs at approximately 10–20 ms, has been associated with water in the myelin sheath (5), and thus provides a measure of the processes of demyelination and remyelination. We recently demonstrated that the magnitude of the short T_2 component correlates very well with the amount of myelin in nerves undergoing degeneration and spontaneous regeneration following traumatic injury of the peripheral nervous system (PNS) (6). Conversely, the MT effect is thought to be mainly mediated by the processes of MT exchange between water and lipid protons within the myelin sheath (7,8). It has been shown (9) that the observed changes in the MT ratio (MTR) and the decrease in the MT macromolecular fraction (M_{0B}) are also a manifestation of the decreased myelin content.

It should be noted, however, that these MR measurements evaluate myelin content as a volume fraction of water (or macromolecules) in myelin, rather than the intra- and extracellular water volumes. Therefore, it is expected that even when there is no myelin loss, the process of inflammation, which results in an increased EM fraction (and therefore increased free water), will produce a decrease in the relative amplitude of the short T_2 component and the MT semisolid fraction, M_{0B}.

The purpose of this study was to measure how the process of inflammation alone affects MR measurements, such as T_1/T_2 relaxation and MT. To achieve this goal, we used an experimental animal model of neural tissue inflammation (10) by injecting tumor necrosis factor alpha (TNF-α) into rat sciatic nerves. This experimental model primarily invokes an inflammatory process with negligible demyelination and axonal loss. The MR parameters were then compared with the results of a quantitative, histomorphometric assessment of inflammation in the adjacent neural tissue. In the light of the current results and data reported in the literature, we also discuss which of the MR measurements is most advantageous for distinguishing inflammation and demyelination.

MATERIALS AND METHODS

Experimental Model of Inflammation

It has been reported (10–13) that when the proinflammatory cytokine tumor necrosis factor-alpha (TNF-α) is injected in small quantities into neural tissue, it induces the process of inflammation within 24 hr. In the first few days

post TNF-α injection, marked inflammatory responses are observed, while axonal degeneration and demyelination are negligible. By 1 week after injection, effects are reported to range from no degeneration or demyelination (12,13) to axonal degeneration, demyelination without axon loss, primary demyelination, and axonal degeneration (10,11). To examine the effects of inflammation on the MR parameters of neural tissue, we measured the MR properties of rat sciatic nerve in vitro 2 days after TNF-α injection in 16 samples. As controls, four untreated samples and four nerve samples with PBS injections (with no TNF-α) were also measured.

Inbred adult male Lewis rats (250–300 g, 10 weeks old, $N = 12$) were obtained from Charles River Canada (St. Constant, QC) and housed in a standard animal facility with 12-hr on/off light conditions. All of the animals were acclimatized prior to surgery and allowed standard rat chow and water ad libitum. All experiments and animal interventions adhered to the guidelines of the Canadian Council on Animal Care. The anesthesia used in all cases consisted of an intramuscular injection of 10 mg/kg xylazine (20 mg/mL; Bayer Inc., Etobicoke, ON) and 100 mg/kg ketamine hydrochloride (0.1 mL/100 g Rogarestic; Rogra-STB, Montreal, QC) into the lumbar paraspinal musculature. For all of the surgical procedures we employed standard microsurgical techniques, using an operating microscope (Wild M651; Wild Leitz, Willowdale, ON). Following induction of anesthesia, the sciatic nerves were exposed via bilateral gluteal and posterior thigh incisions. The injections were made using a microsyringe with a 30-gauge needle. The tip of the needle was carefully inserted subepineurally, and 2 μl of 8000 U/μl rhTNFα were slowly injected. The rhTNFα (Calbiochem, LaJolla, CA) was dissolved in PBS containing 0.1% BSA. Each sciatic nerve was given two injections, spaced 1 cm apart, and the sites of the injections were marked with a superficial epineural 9-0 suture (Dermalon, Davis & Geck; American Cyanamid Co., Danbury, CT). Control injections of PBS containing 0.1% BSA were made in an identical fashion.

Two days later the animals were deeply anesthetized and the sciatic nerves were harvested. The nerve tissue was harvested from both legs after TNF-α PBS injection or no treatment (control samples), as shown in Table 1. Each nerve tissue sample was prepared as shown in Fig. 1. For the MR measurements, the tissue (approximately 1.5 cm long) was harvested around and between the injection sites as one sample, and the entire sample was measured by MRI. Additionally, to ensure continuity in the tissue pathology across the sample, the proximal and distal portions of the injured nerve were evaluated histopathologi-

Table 1
Animals Used in the Study

Animal No.	Left leg	Right leg
1	No injection	PBS
2	PBS	No injection
3	No injection	TNF-α
4	TNF-α	PBS
5	TNF-α	No injection
6	PBS	TNF-α
7–12	TNF-α	TNF-α
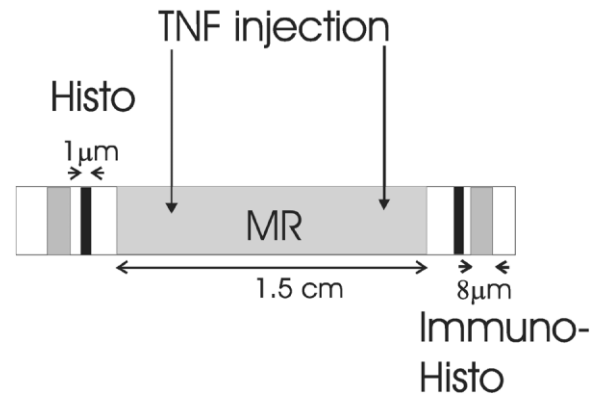
FIG. 1. Schematic of the sciatic nerve segment, the sites of the TNF-α injury, and tissue samples for the MR and histology assessments. The histopathology samples were obtained from both proximal and distal sites. Separate samples were processed for immunohistology and histomorphometry (histo), and the thickness of each section was also noted.

cally (Fig. 1). The pH of TNF-α, normal controls and the nerves before, immediately after, and 2 days postinjection were also measured.

Histopathology

For each distal and proximal portion of the nerve, two histopathological samples were obtained for histomorphometric assessment of the myelin content, axonal integrity, and EM fraction (toluidine blue stain), and for immunohistologic evaluation of the inflammatory process (using antibodies for ED1, a macrophage and monocyte cytoplasmic antigen) (Fig. 1).

For the histomorphometric assessment, the samples were fixed by immersion in universal fixative (40% formalin, 25% glutaraldehyde). They were then postfixed with osmium tetroxide, embedded in epon-araldite, and sectioned on an ultramicrotome (Sorvall MT6000, Kendro, Asheville, NC; or Reichert-Jung Ultracut E, Leica Microsystems, Germany). Toluidine blue was used to stain 1-μm-thick cross sections for light microscopy.

Tissue samples for the immunohistologic assessment were collected, fixed in 10% buffered formalin, and embedded in paraffin. Slides with 8-μm-thick sections were then dewaxed in three changes of xylol, and dehydrated in two changes of 100% ethanol and endogenous peroxidases quenched with a solution of PBS, 0.03% hydrogen peroxide, and 1% sodium azide. Then they were treated with 0.2% pepsin solution in TBS at 37° for 15 min to unmask antigens, and rinsed in tap water. All incubations were performed at room temperature in a humid chamber. The slides were rinsed in PBS and blocked with 7% normal horse serum for 15 min. They were then incubated for 1.5 hr with mouse anti-rat ED1 (1/50 dilution; Chemicon International, Temecula, CA). The sections were washed three times in TBS. Biotinylated horse anti-mouse antibody was added and the samples were incubated for 45 min, and then washed three times with TBS. Commercial avidin/biotin complex (Vector Laboratories, Burlington, ON) was added and the sections were incubated for

40 min, and then washed three times with TBS. Then chromagen solution (NovaRed; Vector Laboratories, Burlington, ON) was added and the sections were incubated for 10 min. Finally, the slides were washed for 5 min in running tap water, and lightly counterstained with hematoxylin.

For quantitative evaluation of neural tissue integrity, a computer-assisted image analysis (CAIA) was performed on the toluidine blue-stained samples using image analysis software (Image-Pro Plus 4.5; Media Cybernetics, Silver Spring, MD). Histomorphometric studies to evaluate the myelin content of each nerve section were performed on randomly selected, representative fields of known area (3093 μm^2), at 1000× magnification on a light microscope (Olympus BX51 light microscope; Olympus America, Inc., Melville, New York). The number of fields evaluated (five to seven) depended on the total cross-sectional sample area, and was selected such that total area evaluated was at least 25% of the total cross-sectional area. Images were captured via a Cool Snap-Pro camera (Media Cybernetics, Inc., Silver Springs, MD) linking the microscope and the image analysis system for further analysis, which involved a three-step approach modeled on the segmentation, recognition, and measurement method of Romero et al. (14), as previously developed in our laboratory (6). Briefly, the evaluation took into account both intact myelin sheaths and myelin present in the form of Wallerian degeneration (WD) profiles or disrupted myelin sheaths (6). The myelin content and extracellular matrix volume (EM) fraction were calculated as percentages of the total sampled area.

MR Measurements

All MR measurements were performed at 20°C and 1.5 T on a 20-cm-bore superconducting magnet (Nalorac Cryogenics Corp., Martinez, CA) controlled by an SMIS spectroscopy console (SMIS, Surrey, UK). Rectangular radiofrequency (RF) pulses were amplified by an RF amplifier (model 3205; American Microwave Technology, Brea, CA). Immediately after tissue excision, the samples were placed in nonprotonated, MR-compatible fluid (Fluorinert; 3M, London, Canada) to avoid dehydration and reduce susceptibility effects. The MR experiments lasted approximately 3 hr. Before and after each experimental session, a multicomponent T_2 decay was measured using a Carr-Purcell-Meiboom-Gill (CPMG) sequence to test the continuity of the sample signal characteristics. The T_2 decay curves varied < 1% during these sessions, which indicated that the samples were stable over the time-course of the MR experiments.

The MR measurements were obtained as follows:

- T_1 relaxation time data were acquired using an inversion recovery (IR) sequence (15) with 35 TI values logarithmically spaced from 1 to 32000 ms, with 10 s between each acquisition and the next inversion pulse, and two averages.
- T_2 relaxation time data were acquired using a CPMG sequence (15,16) with TE/TR = 1/10000 ms, 2000 even echoes sampled, and 100 averages.
- MT-weighted data were measured using a continuous-wave (cw) saturation pulse of 7 s duration. For the standard MTR evaluation, the RF saturation pulse amplitude ($\omega_1/2\pi$) was 670 Hz, and the offset frequency of the saturation (Δ) was 5 kHz. To quantitatively evaluate the MT data (17), seven RF saturation amplitudes ($o_1/2\pi$ = 85, 170, 330, 670, 1330, 2670, and 5340 Hz) and 26 off-resonance frequencies Δ (0.014–250 kHz) were applied. The TR was 10 s, and the number of averages was eight. The effects of any residual transverse magnetization following the off-resonance irradiation was removed by phase-cycling the π/2 pulse (–x/x).

Data Analysis

We analyzed the T_1 data assuming monoexponential behavior. All T_2 decay data were fitted to a multicomponent T_2 model in which the relaxation of each T_2 component had a Gaussian distribution on a logarithmic time scale (6,18). The Gaussian model was found to provide better separation of the T_2 peaks than the commonly used nonnegative least-squares (NNLS) method (19), yet guaranteed approximately the same value of χ^2 and resulted in similar T_2 spectra. Repeated T_2 measurements of a single sample were used to determine that a minimum signal-to-noise ratio (SNR) of 500 was required in order to assess the amplitudes and positions of all three T_2 components with 5% precision.

The MTR was evaluated by the following equation:

$$MTR = \frac{M_0 - M_{SAT}}{M_0},$$ [1]

where M_0 and M_{SAT} denote signal amplitude measured without and with the RF saturation pulse, respectively.

The quantitative MT data were fitted to a "two-pool" model (17) quantifying the exchange between an unrestricted liquid pool and a semisolid macromolecular pool of restricted mobility (20). The model estimates R, the rate of exchange of longitudinal magnetization between liquid and semisolid pools, as well as the dimensionless parameters $1/R_A T_{2A}$, and RM_{OB}/R_A, where R_A is the rate constant of longitudinal relaxation in the liquid pool, T_{2A} is the average transverse relaxation time of the liquid pool, and M_{OB} is the fraction of magnetization that resides in the semisolid pool and undergoes MT exchange.

RESULTS

Histopathology

The histopathology of the control nerves (injected with PBS) showed no signs of inflammation, which was similar to the results in the normal samples. Figure 2 shows representative toluidine blue-stained sections for control (Fig. 2a) and injured nerve (Fig. 2b), as well as the immunohistologic appearance 2 days post TNF-α injection (Fig. 2c). The normal sciatic nerve sample shows well-myelinated axons with adjacent nuclei consisting of mainly Schwann cells (Fig. 2a). In the sciatic nerve 2 days following TNF-α injection, a large number of inflammatory cells (stars) and red blood corpuscles are present. Most axons are well myelinated and appear normal, except for an increased distance between them (increased EM fraction). Occasion-
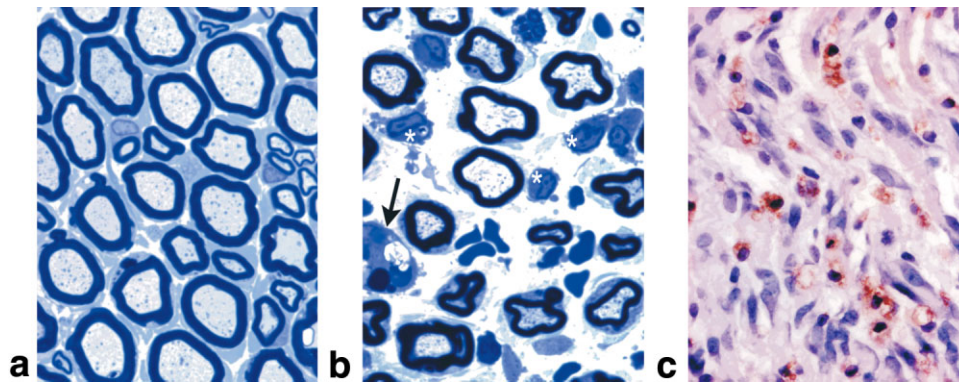
FIG. 2. Toludine blue-stained cross sections of nerves at 1000× magnification. **a:** Normal sciatic nerve sample. The axons are well myelinated, with the occasional Schwann cell present. **b:** Sciatic nerve 2 days after TNF-α injection. Note the large number of inflammatory cells (stars) and red blood corpuscles. Most of the axons are well myelinated and appear normal, except for the increased distance between them. There is an occasional Wallerian degeneration profile (arrow). **c:** ED1-stained longitudinal section counterstained with hematoxylin, 400× magnification. ED1 immunostaining (reddish-brown pigment) reveals a large number of ED1+ macrophages, indicating a marked inflammatory response.

ally, a Wallerian degeneration profile was observed (arrow). The immunohistologic staining (Fig. 2c) revealed the presence of considerable inflammatory cells (ED1+ macrophages and monocytes).

No substantial differences in histopathology between the proximal and distal nerve samples were observed, indicating tissue uniformity across the intervening measured MR samples.

We performed a quantitative assessment with CAIA on the toluidine blue-stained slides, which allowed us to estimate the myelin content and EM fraction (including inflammatory cells). The myelin content of the normal nerves was 31% ± 4%, and was slightly lower in the TNF-α-treated samples (23% ± 7%). The EM fraction substantially increased from 42% ± 2% in untreated nerve to 52% ± 6% for 2 days post TNF-α injection. The larger range of myelin content and EM fraction in the treated samples indicated different degrees of inflammation. The amount of pathology was independent of injection site (left/right leg, $P > 0.6$, $N = 6$, $r = -0.2$); therefore, the samples were treated as independent observations in the comparison between MR parameters and quantitative histopathology.

The pH of the normal sciatic nerves and injected TNF-α solution was 7.4 ± 0.1 and 6.9 ± 0.1, respectively. Two days after injection (just before the nerves were dissected and harvested), the pH of the nerves substantially increased to 8.3 ± 0.1.

MR Parameters

For all measured samples, T_1 relaxation (Fig. 3a) appeared monoexponential, with the average longitudinal relaxation time T_1 for untreated nerves equal to 631 ± 30 ms. T_2 relaxation was multiexponential, showing three well-distinguished T_2 components. The Gaussian fitting procedure yielded values for the T_2 spectrum position, width, amplitude, and relative size of each component. Typical T_2 spectra for normal and TNF-α-treated nerves are shown in Fig. 3b. The T_2 spectrum of normal nerve (solid line) shows three well-distinguished components (centered at

short, intermediate, and long values of T_2), described as follows:

- A short T_2 component at 16 ± 2 ms (average and standard error of the mean for four samples) represented 32% ± 5% of the total curve area.
- An intermediate T_2 component at 42 ± 5 ms, with size 61% ± 1% of the total curve area.
- A long T_2 component at 242 ± 20 ms, with size 11% ± 3% of the total curve area.
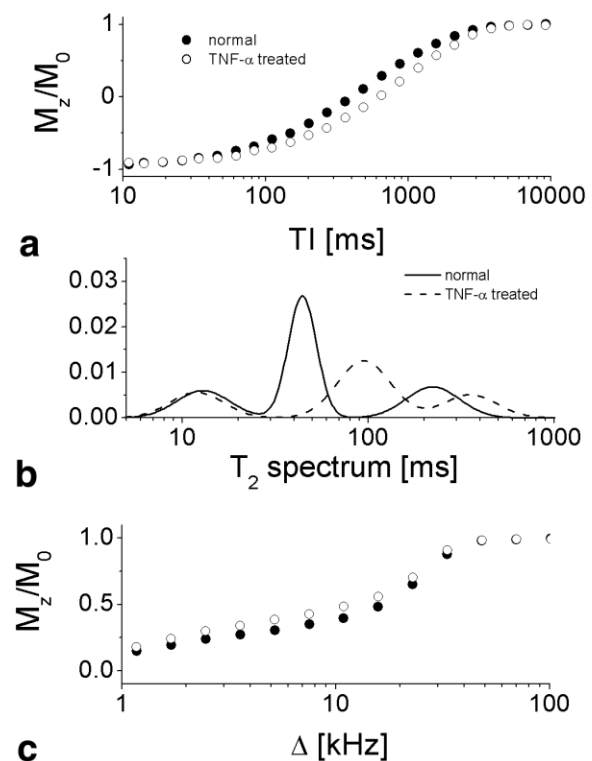
FIG. 3. (**a**) T_1 data, (**b**) T_2 spectrum, and (**c**) MT data for normal and TNF-α-treated samples.

Moreover, the single measure of the T_2 relaxation, $\langle T_2 \rangle$, was evaluated. $\langle T_2 \rangle$ represents an average of the T_2 relaxation spectrum, and is equivalent to the monoexponential estimate of T_2 decay that is usually assessed in clinical MRI. The $\langle T_2 \rangle$ average for the normal nerve was 78 ± 6 ms.

The MTR measured at saturation pulse amplitude $\omega_1/2\pi$ of 670 Hz and the offset frequency of the saturation, Δ, equal to 5 kHz for normal nerves was 0.70 ± 0.01 (Fig. 3c). The two-pool MT model resulted in the MT exchange rate R of 47 ± 4 [s^{-1}] and the fraction of the semisolid pool M_{OB} equal to $10\% \pm 2\%$.

The MR parameters for four PBS-treated samples were similar to those for the control samples. The T_1 relaxation time was 635 ± 28, the average relaxation time $\langle T_2 \rangle$ was 76 ± 6 ms, the value of the intermediate T_2 component was 43 ± 4 ms, the MT exchange R was 46 ± 3 s^{-1}, the semisolid pool fraction M_{OB} was $8\% \pm 1\%$, MTR was 0.69 ± 0.01, and the EM fraction was equal to $42\% \pm 3\%$.

The MR properties of the TNF-α-treated nerves were different from those of the normal and control (PBS-injected) nerves. Figure 3 shows the T_1 data, T_2 relaxation spectrum, and MT data for a normal nerve and a typical TNF-α-injected nerve. The T_1 relaxation time for the TNF-α-treated samples was longer, and the mean for 16 measured samples was 819 ± 80 ms. The T_2 spectrum was also different, as described below:

- The short T_2 component position was approximately the same as for the normal nerve (18 ± 6 ms); however, its percentage of the total area was slightly smaller ($22\% \pm 6\%$).
- The intermediate and long T_2 peak positions were increased, with values of 78 ± 14 ms and 298 ± 39 ms, respectively.
- The average $\langle T_2 \rangle$ relaxation time also increased and was equal to 96 ± 17 ms.

The MT data also showed differences between normal and TNF-α-treated nerves. The MTR was on average lower than that of normal nerves (0.65 ± 4). The semisolid pool M_{OB} decreased to $5\% \pm 2\%$, whereas the MT exchange rate R remained the same at 47 ± 5 [s^{-1}].

To assess whether the changes in the MR parameters mapped onto the observed changes in histopathology, we compared the MR parameters with the quantitative morphometric measure (the EM) of the nerve samples. Figure 4 shows the T_1 (a); the average T_2, $\langle T_2 \rangle$ (b); the value of the intermediate T_2 component (c); the MT semisolid pool fraction. M_{OB} (d); the MT exchange rate constant, R (e); and the phenomenological measure of MT – MTR (f) as a function of the EM fraction for all measured samples. The average relaxation times, T_1 and $\langle T_2 \rangle$, and the value of the intermediate T_2 component increased with the EM fraction. The MT semisolid fraction M_{OB} and the MTR decreased, whereas the MT exchange rate constant R was independent of the EM fraction.

Figure 4 illustrates the substantial correlation (as reflected in the correlation coefficient, r between the measured MR parameters and the histomorphometric assessments of the EM fraction. The errors represent uncertainties in r within a 95% confidence level. It is evident that most of the MR parameters were strongly correlated with histopathology.
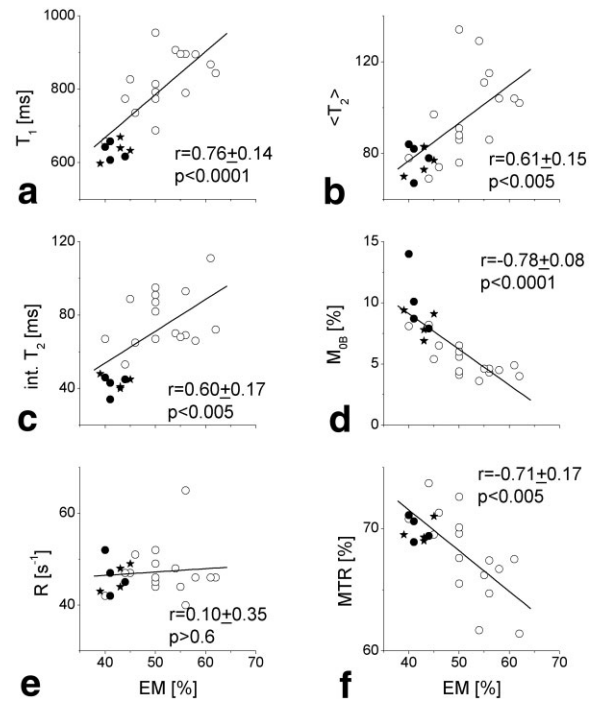
FIG. 4. Correlation between the MR parameters and quantitative measure of the EM fraction. Closed and open circles indicate controls and TNF-α treated samples, respectively. Samples with PBS injections (stars) are also shown.

DISCUSSION

Injecting nerves with TNF-α is an excellent means of inducing inflammation while causing minimal damage to axons and myelin. It is therefore a very useful technique for probing MR contrast mechanisms during neural tissue inflammation. Because of the variability in the histopathological results from the TNF-α-treated samples, it was not feasible to make simple comparisons of mean MR parameters across experimental conditions. Rather, our primary focus was to examine whether the variability in histopathology correlated with the MR measurements. In this study we found more biological variation in the MR parameters and histopathology in the TNF-α-treated samples than in the normal controls. While TNF-α had a significant effect on most of the animals, in some animals it resulted in no apparent inflammation (Fig. 4). This is common in animal models of disease, where the degree of tissue damage is variable across different animals (6). For this reason, instead of comparing the TNF-α-treated samples with the control ones, we correlated the MR measurements for each individual sample to the histopathological results. The TNF-α dose chosen in this study was higher than the usual dose (10). In our pilot studies, lower doses of TNF-α also resulted in inflammation, but produced no effect in approximately 20% of the animals. The 2-day end-point of the study was chosen to maximize the effects of inflammation while minimizing other neural tissue damage. At later time points, demyelination becomes more pronounced (10). The animal model used in this study resulted in a robust inflammatory response.

The current results demonstrate that standard MR techniques, such as average T_1/T_2 relaxation and MTR, correlate strongly with inflammation. This is consistent with observed changes in MRI of a variety of neural system pathologies.

The experimental data presented here describe ex vivo nerve tissue measured at room temperature. Therefore, it is not expected that the extracted MR parameters will have exactly the same values for in vivo neural tissue. T_1/T_2 relaxation times and intercompartmental exchange all increase with temperature (21). However, qualitatively, the MR properties of in vivo tissue are not vastly different from those of excised tissue. In particular, the T_2 spectra of in vivo normal nerves are similar to those obtained in this study (22). Similarly, the quantitative MT parameters for in vivo neural tissue (9) are comparable to those obtained in vitro (20). Thus, it is difficult to believe that in vivo MR measurements will not exhibit similar changes in MR parameters as a result of inflammation.

The quantitative comparison between measured MR parameters and histopathology shows that most of the MR parameters are sensitive to inflammation and may be used as a semiquantitative evaluation of the degree of inflammation. On average, the T_1 and T_2 relaxation times increased by approximately 28% and 25%, respectively, whereas the decrease in MTR was small (approximately 5%). The changes in more quantitative MR measures, such as the value of the intermediate T_2 component (an ~83% increase) and MT macromolecular fraction M_{OB} (an ~50% decrease) are more pronounced. Other MR parameters, such as the relative curve areas of the T_2 components, spectra change only slightly with inflammation. Interestingly, the MT exchange rate R appears to be independent of inflammation. The moderate change in MTR due to inflammation may be explained by conflicting contributions of the MT and direct effects on the MTR. It has been shown that MTR is proportional to the RM_{OB}/R_A ratio (23). In the case of inflamed nerves, the decrease in MTR caused by decreased M_{OB} is counteracted by a decreased longitudinal relaxation rate R_A.

In most neural tissue pathologies, the process of inflammation is accompanied by nervous tissue damage, demyelination, and axonal loss. It is generally believed that the ability to differentiate these processes may be of great value to researchers in elucidating the pathobiology of nervous system disorders and assessing response to therapeutic interventions. For example, we have shown that rat sciatic nerves that can spontaneously regenerate following traumatic injury are on average more inflamed than those with irreversible structural changes (6). However, it is very difficult to distinguish between inflammation and demyelination using standard MR techniques. This is because the changes in the MR signal intensities in the standard (clinically used) T_1-, T_2-, and MT-weighted images due to inflammation are very similar to those related to myelin loss. However, it may be possible to make such a distinction by analyzing quantitative MR measures. Although the process of demyelination increases T_1/T_2 relaxation times and decreases the MT parameters, there are some fundamental differences. We have shown that a total loss of myelin in WM (24) should result in a T_1 relaxation increase of approximately 20% and an average T_2 increase

of 30%. The changes in the T_1 relaxation are caused mainly by decreased MT effect, whereas a decrease in the average T_2 is caused primarily by the disappearance of the short T_2 component (associated with myelin). The shift in the value of the intermediate T_2 component, in the case of total myelin loss, is also anticipated, due to the processes of intercompartmental exchange, but it should not exceed 30%. Our previous study (24) of MT and T_2 in WM demonstrated that full myelin loss would result in significant decrease in the semisolid macromolecular pool, M_{OB}, to ~2% (the protein part of the macromolecular pool in the intra- and extracellular compartments). Consequently, MTR would also drastically decrease to about 0.4. In the current study, we observed much higher increases with moderate inflammation in the average T_1/T_2 relaxation, but smaller changes in the MTR.

The most effective way to distinguish inflammation from myelin loss is to analyze the T_2 spectrum. In the case of demyelination, the relative area of the short T_2 component should drastically decrease, while in the process of inflammation the value of the intermediate component substantially increases. In the present study, the amplitude of the short T_2 component was observed to decrease with inflammation; however, the changes were moderate and were accompanied by a huge shift of the intermediate component. The short T_2 component decrease in the case of inflammation is expected, since inflammation results in an increased EM in water. Therefore, the relative myelin component may slightly decrease. However, the change is relatively small (approximately 20–30%). In the case of demyelination, only a much larger decrease in the amplitude of the short T_2 component is anticipated (24), and a much smaller shift in the intermediate T_2 should be present.

The MT results are also interesting, since they defy commonly-held beliefs. Given the interactions that occur between water and protons associated with myelin lipids, it is assumed that most of the MT effect occurs in myelin, and consequently that MT would be a perfect measure of the process of demyelination. Therefore, it is surprising that such a significant decrease in the macromolecular fraction M_{OB} was observed in this study. It is expected that the M_{OB} would slightly decrease with an increase in the EM fraction. M_{OB} is the relative measure of the macromolecular proton population that takes an active part in the MT process. M_{OB} is defined as a fraction of the semisolid pool in comparison to that of liquid water. Since the process of inflammation results in increased extramyelin water, M_{OB} should decrease. However, the slight increase in free water (by approximately 15%) observed in this study should result in M_{OB} by approximately the same amount. Therefore, it is anticipated that M_{OB} should decrease from 10% (for normal nerve) to approximately 8% in the presence of inflammation. However, we observed much smaller M_{OB} values (~5%) in the case of inflamed nerves. The origins of this effect are not fully understood; however, there are several reasons for such a large M_{OB} change. It is possible that the inflammatory cells (including macrophages) that are present in the nerve block the MT sites from the active MT exchange. Moreover, we observed a significant change in the pH of the inflamed nerves. It has been shown that MT effects are very sensitive to the pH of

Table 2
Trends in the MR Parameters Due to Myelin Loss or Inflammation

MR parameter	Demyelination	Inflammation
T_1	++	+++
$<T_2>$	++	+++
Amplitude of short T_2 component	− − −	−
Position of intermediate T_2 component	+	+++
M_{0B}	− − −	− −
MTR	− − −	−

the sample. In particular, for multivesicle lipid bilayers, the maximum MT effect occurs at approximately low pH values (5–6), drastically decreasing (by 200%) with pH at 8. The changes in pH are related to the processes of inflammation, rather than to the TNF-α injection. Our preliminary studies also showed that the nerve pH increases in the case of Wallerian degeneration induced by crush injury. Therefore, the macromolecular fraction M_{0B} may not be the best indicator of demyelination if inflammation is also present. It should be noted, however, that the anesthesia might also have influenced the pH of the nerve.

Table 2 summarizes the trends in MR parameters that are anticipated from the processes of severe demyelination and inflammation. Although these trends occur in the same direction, the magnitudes by which the MR parameters change are substantially different, which enables us to distinguish between myelin loss and inflammation. Quantitative MR techniques, such as multicomponent T_2 relaxation and MT, are available in vivo (5,9,25); however, because of the time limitations of clinical scanners, they are rarely performed. In clinical MR examinations, the standard techniques may still be able to distinguish between inflammation and demyelination by the different degrees of change in T_2 relaxation and MTR. For example, a T_2 increase with a significant MTR decrease would be consistent with demyelination, whereas even a large T_2 increase with a moderate MTR decrease would suggest inflammation.

CONCLUSIONS

Most MR parameters change in the presence of neural tissue inflammation. Multicomponent T_2 relaxation is the best means of distinguishing between the processes of inflammation and myelin loss. The quantitative measurement of MT is less successful due to competing contributions from demyelination and pH-sensitive changes in the MT effect.

ACKNOWLEDGMENT

REFERENCES

1. Moore G. MRI—clinical correlations: more than inflammation alone—what can MRI contribute to improve the understanding of pathological processes in MS? J Neurol Sci 2003;206:175–179.
2. Schroeter M, Franke C, Stoll G, Hoehn M. Dynamic changes of magnetic resonance imaging abnormalities in relation to inflammation and glial responses after photothrombotic cerebral infarction in the rat brain. Acta Neuropathol 2001;101:114–122.
3. Stoppe G, Staedt J, Brunhn H. Resonance-imaging—value for the (differential) diagnosis of dementia of the Alzheimer-type and vascular dementia. Fortschr Neurol Psychol 1995;63:425–440.
4. Nosaka K, Clarkson P. Changes in indicators of inflammation after eccentric exercise of the elbow flexors. Med Sci Sports Exer 1996;28:953–961.
5. MacKay AL, Whitall KP, Adler J, Li DKB, Paty DW, Graeb D. In vivo visualisation of myelin water in brain by magnetic resonance. Magn Reson Med 1994;31:673–677.
6. Webb S, Munro C, Midha R, Stanisz G. Is multicomponent T-2 a good measure of myelin content in peripheral nerve? Magn Reson Med 2003;49:638–645.
7. Koenig S. Cholesterol of myelin is the determinant of gray-white contrast in MRI of the brain. Magn Reson Med 1991;20:285–296.
8. Fralix T, Ceckler T, Wolff S, Simon S, Balaban R. Lipid bilayer and water proton magnetization transfer—effect of cholesterol. Magn Reson Med 1991;18:214–223.
9. Sled JG, Pike GB. Quantitative imaging of magnetization transfer exchange and relaxation properties in vivo using MRI. Magn Reson Med 2001;46:923–932.
10. Redford EJ, Hall SM, Smith K. Vascular changes and demyelination induced by the intraneural injection of tumour necrosis factor. Brain 1995;118:869–878.
11. Hall SM, Redford EJ, Smith KJ. Tumour necrosis factor-a has few morphological effects within the dorsal columns of the spinal cord, in contrast to its effects in the peripheral nervous system. J Immunol 2000;106:130–136.
12. Spies J, Westland K, Bonner J, Pollard J. Intraneural activated T-cells cause focal breakdown of the blood-nerve barrier. Brain 1995;118:857–868.
13. Uncini A, Di Muzio A, Di Guglielmo G, De Angelis M, De Luca G, Lugaresi A, Gambi D. Effect of rhTNF-alpha injection into rat sciatic nerve. J Neuroimmunol 1999;94:88–94.
14. Romero E, Cuisenaire O, Denef J, Macq B. Automatic morphometry of nerve histological sections. J Neurosci Methods 2000;97:111–122.
15. Carr H, Purcell E. Effects of diffusion on free precession in nuclear magnetic resonance experiments. Phys Rev 1954;94:630–638.
16. Meiboom S, Gill S. Modified spin-echo method for measuring nuclear relaxation times. Rev Sci Instrum 1958;29:688–691.
17. Henkelman RM, Huang X, Xiang Q-S, Stanisz GJ, Swanson SD, Bronskill MJ. Quantitative interpretation of magnetization transfer. Magn Reson Med 1993;29:759–766.
18. Stanisz GJ, Henkelman RM. Diffusional anisotropy of T2 components in bovine optic nerve. Magn Reson Med 1998;40:405–410.
19. Whittall KP, MacKay AL. Quantitative interpretation of NMR relaxation data. J Magn Reson 1989;95:134.
20. Morrison C, Stanisz GJ, Henkelman RM. Modeling magnetization transfer for biological-like systems using a semi-solid pool with a super-Lorentzian lineshape and dipolar reservoir. J Magn Reson B 1995;108:103–113.
21. Stanisz GJ, Li JG, Wright GA, Henkelman RM. Water dynamics in human blood via combined measurements of T2 relaxation and diffusion in the presence of gadolinium. Magn Reson Med 1998;39:223–233.
22. Does MD, Gore JC. Compartmental study of T-1 and T-2 in rat brain and trigeminal nerve in vivo. Magn Reson Med 2003;47:274–283.
23. Henkelman RM, Stanisz GJ, Graham JS. Magnetization transfer in MRI: a review. NMR Biomed 2001;14:57–64.
24. Stanisz GJ, Kecojevic A, Bronskill MJ, Henkelman RM. Characterizing white matter with magnetization transfer and T2. Magn Reson Med 1999;42:1128–1136.
25. Tozer D, Ramani A, Barker GJ, Davies GR, Miller DH, Tofts PS. Quantitative magnetization transfer mapping of bound protons in multiple sclerosis. Magn Reson Med 2003;50:83–91.